Differential chromatin accessibility between pre- and post-natal stages highlights putative causal regulatory variants in pig skeletal muscle

Ervin Shishmani[a], Andrea Rau[b], Sarah Djebali[c], Emily L. Clark[d#], Jordi Estellé[b], Valentino Palombo[a], Mariasilvia D'Andrea[a], Elisabetta Giuffra[b]

[a]Dipartimento Agricoltura, Ambiente e Alimenti, Università degli Studi del Molise, Campobasso, Italy.
[b]Université Paris-Saclay, INRAE, AgroParisTech, GABI Jouy-en-Josas, France.
[c]IRSD, Université de Toulouse, INSERM, INRAE, ENVT, Univ Toulouse III - Paul Sabatier (UPS), Toulouse, France.
[d]The Roslin Institute, The Royal (Dick) School of Veterinary Studies, Easter Bush Campus, Midlothian, UK.

[#]Current Address: The European Molecular Biology Laboratory's European Bioinformatics Institute, Wellcome Genome Campus, Hinxton, Cambridge, UK.

Abstract

The dynamics of chromatin patterns underlie the developmental programmes of body tissues. Deciphering how these dynamics modulate the effect of regulatory variants on agronomically important traits across developmental stages remains largely unexplored in farmed animals.

In this work, we focused on the skeletal muscle. We integrated chromatin accessibility, molecular QTL and GWAS data to identify developmental stage–specific regulatory elements and to highlight putative causal regulatory variants underlying complex traits.

To define stage-differential open chromatin regions in the skeletal muscle, we aggregated 202 publicly available ATAC-seq libraries, from four different studies, spanning fetal and postnatal (piglet) stages, processed them through the nf-core ATAC-seq pipeline, obtained the consensus peaks, and performed differential accessibility analysis. We aggregated 202 publicly available ATAC-seq libraries, from four different studies, spanning fetal and postnatal (piglet) stages, processed them through the nf-core ATAC-seq pipeline, obtained the consensus peaks, and performed differential accessibility analysis. These peaks were systematically intersected with five classes of cis-acting molecular QTLs (molQTLs) from the PigGTEx resource, followed by functional enrichment analysis, promoter-focused functional annotation, and integration with gene–trait pairs. Finally, we intersected the eGenes (i.e., genes whose expression is regulated by at least one cis-eQTL) to link variants previously associated with QTLs for production traits.

We identified 132,275 differentially accessible peaks (DAPs) separating fetal from piglet muscle. Fetal DAPs were enriched in promoter and intergenic regions, whereas piglet DAPs were enriched in intronic regions, plausibly reflecting a shift from transcriptional priming to postnatal regulatory refinement. Across all molQTL classes, overlaps with accessible regions were highly significant ($p < 0.001$). The top 25% strongest effect variants were enriched within DAPs, exhibiting promoter–TSS enrichment in fetuses and intronic enrichment in piglets, with the top 1% of eQTLs predominating in the fetal stage (14 fetal vs. 4 piglet). Gene Ontology analysis of promoter-accessible eGenes revealed prenatal enrichment for RNA metabolism and chromatin organization, contrasting with the postnatal enrichment for muscle contraction and lipid metabolism. Finally, the intersection of promoter

eGenes with previously colocalized growth, muscle, and reproductive traits identified 107 fetal-stage and 30 piglet-stage associated regulatory elements, with only three eGenes shared between stages.

Together, these findings demonstrate that combining stage-differential chromatin accessibility and regulatory variants provides pertinent information for prioritizing putative causal variants to refine precision breeding strategies for complex traits in pigs.

Keywords

Porcine skeletal muscle, ATAC-seq, Chromatin accessibility, Differentially accessible peaks (DAPs), Molecular QTLs (molQTLs), Promoter-TSS, Regulatory variants, Complex traits

1. Introduction

The development of skeletal muscle is a complex biological process that plays a crucial role in pig production, influencing meat yield, carcass quality, and overall commercial value (Sosnicki, A et al., 2025). Muscle traits such as fiber number, size, type, and intramuscular fat content are key determinants of growth efficiency and meat quality, making the identification of their underlying regulatory mechanisms essential for improving pig breeding programs (Cho et al., 2019).

Myogenesis, the process of muscle formation, is controlled by a tightly regulated network of genetic and epigenetic factors, including chromatin accessibility, transcription factors, and cis-regulatory elements (Lin et al., 2023). The functional genome of skeletal muscle has been extensively annotated in livestock species, including pigs (Harrison et al. 2024). Among these annotations, the Assay for Transposase-Accessible Chromatin with sequencing (ATAC-seq) allows for the identification of open chromatin regions (OCRs) that are associated with active regulatory elements (Buenrostro et al., 2013). Recent studies have used ATAC-seq to investigate the regulatory landscape of porcine muscle development, highlighting dynamic changes in chromatin accessibility between fetal and postnatal stages (Miao et al., 2021; Yue et al., 2021; Salavati et al., 2022; Feng et al., 2023; Chalabi et al. 2025). For example, Salavati et al. (2022) identified over 4,600 differentially accessible regions in pig semitendinosus muscle, many of which were linked to genes involved in myogenesis and muscle growth. These findings underscore the importance of integrating chromatin accessibility data with genetic variation to gain insights into the fine regulation of muscle-associated traits.

Genome-wide association studies (GWAS) have identified numerous genomic loci associated with muscle growth, carcass composition, and meat quality traits in pigs (Crespo-Piazuelo et al., 2021). However, pinpointing causal variants and regulatory mechanisms within these loci remains a major challenge. The availability of several expression quantitative trait loci (eQTLs) datasets provides a valuable resource for linking genetic variation to gene expression in farm animal species (Fang et al. 2025). The PigGTEx project (http://piggtex.farmgtex.org) has cataloged tens of thousands of cis-eQTLs and eGenes (i.e., genes whose expression is regulated by at least one cis-eQTL) across multiple pig tissues, offering insights into tissue-specific gene regulation (Teng et al., 2024). Beyond eQTLs, the PigGTEx project has characterized additional molecular quantitative trait loci (molQTLs) across 34 tissues, including skeletal muscle. These molQTLs include splicing QTLs (sQTLs), exon expression QTLs (eeQTLs), enhancer QTLs (enQTLs), and long non-coding RNA QTLs (lncQTLs), providing a multi-layered view of genetic regulatory variation across tissues.

The objective of the present study was to identify developmental stage–specific regulatory elements in the pig skeletal muscle and to highlight putative causal regulatory variants underlying complex traits. A scheme of the analytical workflow is provided in **Figure 1**. We first generated a comprehensive chromatin accessibility resource for porcine skeletal muscle by aggregating and reprocessing four publicly available ATAC-seq datasets spanning the fetal and postnatal developmental stages. This cross-study integration not only increased sample size but also expanded breed diversity and developmental coverage, thereby enabling the identification of more robust and generalizable consensus peaks and DAPs (Differentially Accessible Peaks). We then integrated both consensus peaks and DAPs with the comprehensive set of cis-acting skeletal muscle molQTLs from the PigGTEx project (Teng et al., 2024) and applied gene set enrichment analysis (GSEA) to interpret the functional programs associated with eGenes. We further examined the DAPs at promoter–TSS (transcription start sites) overlapping the strongest eQTLs to assess how the accessibility shifts at these sites occurred in fetal and piglet muscle. In addition, we tested the enrichment and genomic distribution across fetal and post-natal stages of the strongest effect variants (top 25% of each molQTL class) within these DAPs.

Finally, we incorporated the gene–trait colocalization results derived from a large-scale integrative GWAS framework developed by Xu et al. (2025). This framework combines transcriptome-wide association studies (TWAS), summary-based Mendelian randomization (SMR), and Bayesian colocalization to identify loci where gene expression and trait variation likely share a common causal variant. By intersecting these colocalized gene–trait associations with promoter-accessible eGenes, we highlighted 107 fetal-stage and 30 piglet-stage regulatory elements associated with complex traits.

Through this multi-layered integration of functional genomic, regulatory QTL, and trait association data, our study provides new insights into the dynamics of chromatin accessibility of skeletal muscle during development and provides pertinent information for prioritizing putative causal variants to refine precision breeding strategies for complex traits in pigs.

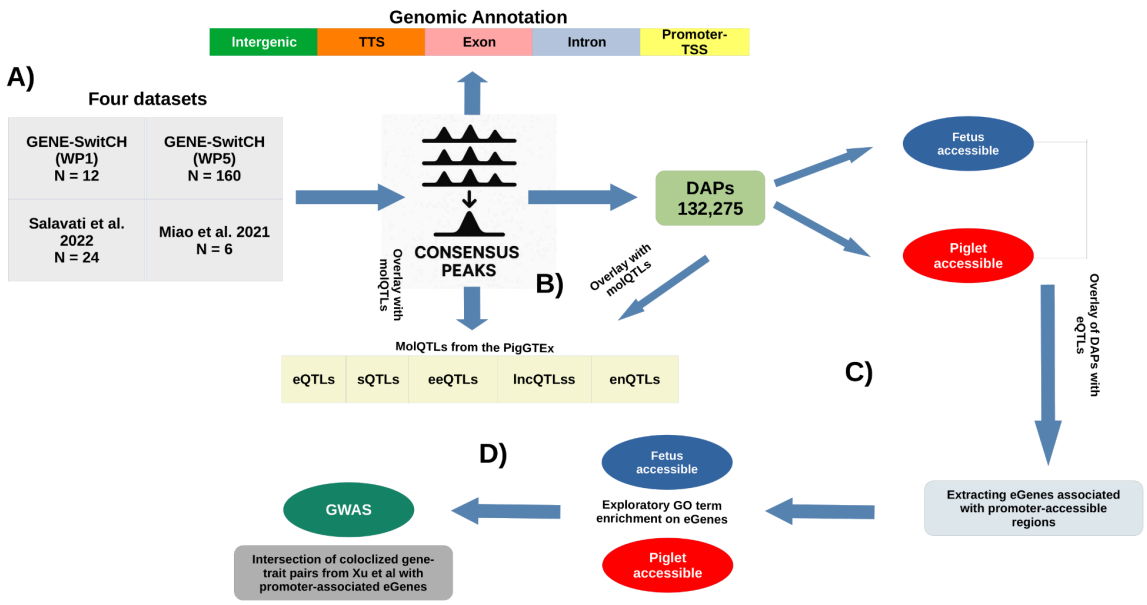

Figure 1. Schematic overview of the analytical workflow.

A) Publicly available ATAC-seq datasets were aggregated to generate consensus peaks, followed by genomic annotation and differential accessibility analysis to identify stage-specific DAPs. **B)** Consensus peaks and DAPs were integrated with cis-molQTLs from PigGTEx. **C)** eGenes associated to promoter eQTLs located inside DAPs were subjected to GO enrichment analysis and **D)** intersected with colocalized GWAS gene–trait pairs to identify developmental stage–specific regulatory elements linked to gene expression and complex traits in porcine skeletal muscle.

2. Materials and methods

2.1. ATAC-seq dataset collection and harmonization

To investigate open chromatin dynamics in porcine skeletal muscle development, a total of 202 muscle ATAC-seq libraries (110 fetal and 92 piglet samples; 124 male, 78 female) were compiled and harmonized from four publicly available datasets (Suppl. Table 1). These datasets were systematically identified through the FAANG Data Portal and ENA repositories. Datasets were included if they provided raw FASTQ files for the skeletal muscle tissue collected at fetal and/or postnatal stages and were generated using standard ATAC-seq protocols. At the time of the search, only these four datasets fulfilled these criteria, with other datasets being excluded due to different target tissues, inaccessible raw data, or insufficient metadata for integration.

The first two datasets were obtained from the FAANG data portal (https://data.faang.org/projects/GENE-SWitCH) as part of the GENE-SWitCH project. The GENE-SWitCH WP1 dataset (https://data.faang.org/dataset/PRJEB44468) includes 12 biological replicates from four Large White pigs, sampled at prenatal days 30 and 70 and at the newborn stage. The GENE-SWitCH WP5 dataset consists of 160 biological replicates from the progeny of TN60/TN70 sows and Duroc/Tempo boars, sampled at prenatal day 70 and 10 weeks postnatal (Chalabi et al.,

2025). The third FAANG dataset (https://data.faang.org/dataset/PRJEB41485), published by Salavati et al. (2022), comprises 24 Large White × Landrace crossbred pigs, with samples collected at multiple prenatal and postnatal time points (prenatal: 45, 60, 90 days and postnatal: 1 week, 6 weeks). The fourth dataset (NCBI GEO; GSE180840), from Miao et al. (2021), includes muscle samples from Luchuan and Duroc pigs at 180 days of age with a sample size of 6 biological replicates. Although the WP5 dataset provided the majority of samples, incorporating additional datasets expanded breed diversity and developmental time points, thereby reducing study-specific biases.

In all cases, libraries were prepared using Illumina NovaSeq sequencing. For downstream analyses, all sampling time points were retained and datasets were merged and categorized into two broad developmental stages (fetus and piglet) due to the strong imbalance of sample sizes across time points.

2.2. Alignment and peak calling of compiled ATAC-seq data

Raw sequencing reads from the compiled ATAC-seq datasets were processed using version 1.2.1 of the nf-core ATAC-seq pipeline (Ewels et al., 2020) (https://nf-co.re/atacseq). Reads were aligned to the Sus scrofa 11.1.108 reference genome using BWA (Li & Durbin, 2009), and quality control metrics were assessed within the pipeline.

For peak calling, MACS2 (Zhang et al., 2008) was used to identify OCRs in each group. Peaks detected within each stage were merged to generate consensus peak sets. Annotation of consensus peaks was performed using HOMER (Heinz et al., 2010), assigning peaks to genes either by transcription start site (TSS) overlap or proximity to the nearest gene. Peak quantification was performed using Subread featureCounts to count the number of aligned reads overlapping consensus peak regions identified by MACS2 across samples, generating a count matrix which was used for normalization and differential accessibility analyses. Mitochondrial peaks were removed as artifacts before downstream analyses.

2.3. Normalization and differential accessibility analysis

To correct for non-linear trended efficiency biases, loess normalization was applied to peak counts using the csaw Bioconductor package (Lun & Smyth, 2016). Principal component analysis (PCA) was performed on log-normalized accessibility data to visualize genome-wide variation between the two developmental stages (Suppl. Figure 1).

Peaks with globally weak accessibility were filtered out, retaining only those with greater than 10 counts per million (CPM) in at least 10 samples. Differential accessibility analysis was performed on log-normalized CPM values using the limma-voom approach (Liu et al., 2015). Empirical sample quality weights were included to account for experimental biases that systematically affected variability for all or most of the peaks in a given sample. For each peak, a linear model was fitted, with sex and developmental stage as fixed factors, and experiment (dataset source) as a random factor to account for batch effects. Contrasts were estimated to test for differential accessibility between developmental stages (piglets vs fetuses) and sexes (males vs females).

Multiple testing correction was performed using the Benjamini-Hochberg procedure, with a false discovery rate (FDR) threshold of 5% to identify statistically significant DAPs.

2.4. Integrative analysis of ATAC-seq peaks and cis-molQTLs

Annotated ATAC-seq peaks were integrated with multiple types of cis-acting molQTLs from the PigGTEx project (Teng et al., 2024). For each type of molQTL (eQTLs, sQTLs, eeQTLs, enQTLs, lncQTLs) in skeletal muscle, cis-molQTLs were identified using a window of ±1 Mb around the TSS of the corresponding gene. Significant cis-molQTLs were defined using an FDR threshold of < 0.05, implemented as a Local False Sign Rate (LFSR) < 0.05.

To identify overlapping genomic regions between ATAC-seq peaks and cis-molQTLs, analyses were conducted using the GenomicRanges (version 1.58.0) package in R (Lawrence et al., 2013). No minimum overlap threshold was applied, meaning peaks and cis-molQTLs overlapping by even a single base pair were considered to be a valid intersection. The same approach was used to identify overlaps between DAPs and cis-molQTLs. The results of the overlaps are shown in Table 1.

For eQTLs specifically, promoter–TSS overlaps were examined in more detail. We ranked variants by absolute effect size and selected the top 1% strongest eQTLs. Among these, only those falling within promoter–TSS DAPs were retained. We then quantified their logFC in accessibility between stages to assess whether the strongest regulatory variants preferentially coincided with fetal or piglet promoters.

Beyond promoters, we assessed whether strong-effect variants across all molQTL classes were preferentially enriched within DAPs. Strong variants were defined as the top 25% of each molQTL class based on absolute effect size. Enrichment was tested using Fisher's exact test, comparing strong versus non-strong variants inside versus outside DAPs. Finally, we stratified these strong variants by genomic category (intergenic, TTS, exon, intron, promoter–TSS) to evaluate their developmental distribution between fetal and piglet muscle.

2.5 Integration with trait–gene colocalization data

We integrated our ATAC-seq results with the trait–gene colocalization data generated by Xu et al. (2025). Xu et al. combined transcriptome-wide association studies (TWAS), summary-data Mendelian randomization (SMR), and Bayesian colocalization to identify loci where gene expression and phenotypic variation likely share a causal variant. They retained only gene–trait pairs with regional colocalization probability (RCP) > 0.5. The trait set comprised two complementary meta-analytical designs: (i) cross-breed meta-analyses for 232 traits based on 2,056 high-quality GWAS summary statistics across 59 pig populations (labeled M_), and (ii) breed-specific meta-analyses for 12 traits in Duroc (D_), Landrace (L_), and Yorkshire (Y_) pigs, capturing lineage-specific effects (Xu et al. 2025).

We intersected these trait-associated genes with the stage-specific eGenes associated with accessible promoter regions identified in our ATAC-seq analysis, enabling us to link chromatin accessibility to trait-associated gene regulation in pig skeletal muscle.

2.6 Gene set enrichment analysis (GSEA)

We performed Gene Ontology (GO) enrichment analysis to explore the biological processes associated with promoter-accessible eGenes linked to cis-eQTLs in fetal and piglet muscle. Enrichment analysis was conducted separately for genes associated with peaks of increased

accessibility in fetuses and those with increased accessibility in piglets using the DAVID Functional Annotation Tool (Huang et al., 2009). We focused on GO Biological Process categories with uncorrected p-values < 0.05, fold enrichment > 1.5, and a minimum of three genes per term to identify potential functional trends within each developmental stage. The background gene list was set to the default background in DAVID.

3. Results

3.1 Compiled chromatin accessibility landscape in porcine skeletal muscle

To characterize the chromatin accessibility profile of porcine skeletal muscle, open chromatin regions were identified from ATAC-seq data generated across 202 muscle samples, including 110 fetuses and 92 piglets (Suppl. Table 1). The datasets were merged and grouped into two broad developmental stages: fetal and piglet. Sequencing reads from the combined dataset were aligned to the reference pig genome, and OCRs were subsequently identified.

Genome-wide chromatin profiling had identified a total of 170,978 consensus peaks. Genomic annotation of the consensus peaks showed that 80,676 were located in intronic regions, 62,225 in intergenic regions, 12,896 in exons, 10,429 in promoter-TSS regions, and 4,048 in transcription termination site regions (Figure 2; Suppl. Table 2). This distribution was consistent with the expected positioning of cis-regulatory elements in the pig and other mammal genomes (Bai et al., 2023; Alexandre et al., 2021). The read distribution profiles around transcription start sites (TSS) showed a strong enrichment at the TSS and upstream regions (Suppl. Figure 1), consistent with expected patterns of promoter-associated chromatin accessibility (Miao et al., 2021).

PCA was performed on normalized chromatin accessibility profiles for consensus peaks to explore global variation across samples (Suppl. Figure 2). The PCA revealed mild stratification according to the dataset origin, indicating small but detectable batch-associated effects across experiments. As expected and as shown in previous work (Chalabi et al., 2025), no clear separation was observed between male and female samples. In contrast, fetal and piglet samples were clearly separated along the first principal component, confirming the widespread developmental differences in chromatin accessibility patterns previously observed (Chalabi et al., 2025).

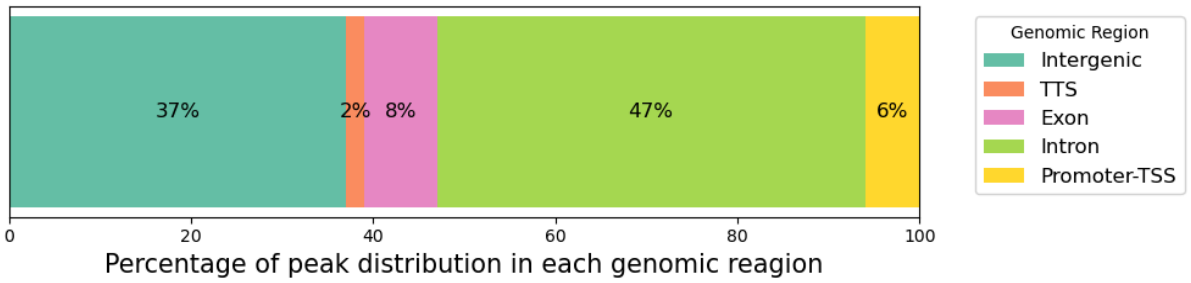

Figure 2. Genomic annotation of consensus ATAC-seq peaks in porcine skeletal muscle. The plot shows the distribution of 170,978 consensus peaks across major genomic regions, annotated using HOMER. The majority of peaks are located in intronic (47%) and intergenic (37%) regions, with

smaller proportions mapping to exons (8%), promoter-TSS regions (6%), and transcription termination sites (2%).

3.2 Differential chromatin accessibility between fetal and piglet muscle

To identify DAPs between the fetal and piglet muscle, differential accessibility analysis was conducted between fetal and piglet samples using the limma-voom framework with empirical quality weights. After excluding peaks on sex chromosomes, a total of 132,275 significant DAPs between developmental stages were identified at an FDR threshold of 0.05. Among these, 70,756 peaks exhibited increased accessibility in fetal muscle, while 61,519 were more accessible in piglet muscle. Each differentially accessible peak was thus assigned to the developmental stage in which it was more accessible. Note that this classification reflected statistically significant differences in accessibility, rather than mere presence or absence of signal.

Genomic annotation revealed that DAPs followed a distribution similar to the consensus peaks, with the majority located in intronic and intergenic regions. However, stage-specific differences in chromatin accessibility were evident (Figure 3; Suppl. Table 3). Peaks more accessible in fetal samples were more frequently located in intergenic regions (28,654 vs. 18,764) and promoter-TSS regions (5,786 vs. 2,556), whereas piglet-associated peaks were found in majority in intronic regions (34,239 vs. 29,525) as shown in Suppl. Table 3.

These results highlighted a developmentally stratified chromatin accessibility landscape in porcine muscle, with distinct classes of regulatory elements engaged across fetal and postnatal stages.

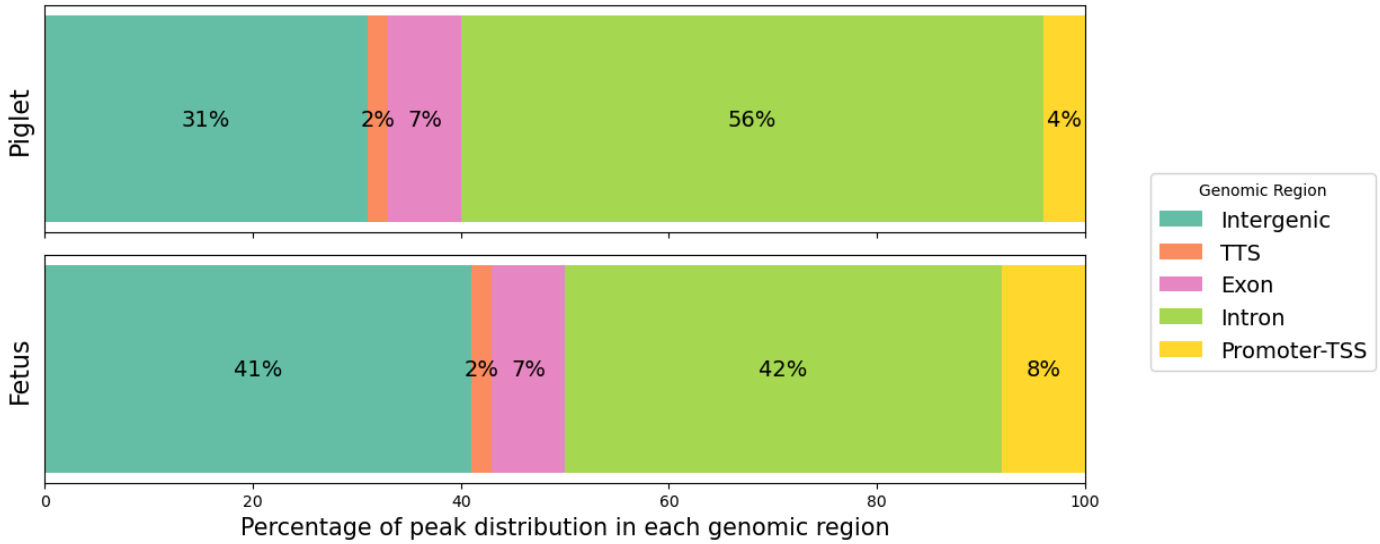

Figure 3. Genomic distribution of differentially accessible peaks (DAPs) between fetal and piglet skeletal muscle. Stacked bar plots show the percentage of DAPs located in intergenic, intronic, exonic, promoter–TSS, and transcription termination site (TTS) regions for each developmental stage.

3.3 Integration of chromatin accessibility and molecular QTLs

3.3.1 Integration of ATAC-seq consensus peaks with molQTLs

To investigate the regulatory potential of accessible chromatin in porcine skeletal muscle, we explored the overlap between chromatin accessibility and the datasets of cis-acting molQTLs (Teng et al., 2024). Supplementary Table 4 provides a summary of the skeletal muscle cis-molQTLs, the total number of variants and their overlaps with consensus ATAC-seq peaks and DAPs at the fetal and piglet stages.

Muscle-specific cis-molQTLs were identified by associating genetic variants with proximal molecular traits to identify context-dependent regulatory variants that mechanistically link genotype to transcriptional regulation.

We first intersected molQTLs and consensus ATAC-seq peaks (Figure 4, Suppl. Table 5A). Among the 162,807 consensus peaks, 60,554 (37.2%) overlapped with 343,496 cis-eQTL variants, corresponding to 33,938 unique eGenes. The distribution of cis-eQTL-overlapping peaks roughly reflected that of genomic annotation regions: intronic (19.4%) and intergenic (9.0%) were most frequent, followed by exonic (3.9%), promoter-TSS (3.7%), and TTS (1.4%) regions. A total of 50,150 (30.8%) consensus peaks overlapped with 275,864 sQTL variants, with similar genomic distributions: intronic (16.4%), intergenic (7.2%), exonic (3.4%), promoter-TSS (3.3%), and TTS (1.2%) peaks. Enhancer QTLs (enQTLs) were found in 23,530 (14.5%) consensus peaks, overlapping 107,021 variants, primarily in intronic (7.3%) and intergenic (3.2%) regions. For exon expression QTLs (eeQTLs), 58,744 (36.1%) consensus peaks overlapped with 327,363 variants, again enriched in intronic (18.8%) and intergenic (8.4%) contexts. Lastly, 34,944 (21.5%) consensus peaks overlapped with 160,339 lncQTL variants, with the highest representation in intronic (11.0%) and intergenic (5.0%) regions (Suppl. Table 5A).

To statistically assess whether the observed overlaps exceeded random expectation, we performed a permutation-based enrichment analysis. For each molQTL class, we generated 1,000 randomized sets of peak coordinates preserving peak count, length, and chromosomal assignment. The number of overlapping molQTL variants was computed for each permutation to derive a null distribution. For all the eQTLs (343,496), sQTLs (275,864), eeQTLs (327,363), enQTLs (107,021), and lncQTLs (160,339), the observed number of overlapping variants was significantly greater than expected by chance (empirical $p < 0.001$).

Together, these results highlighted a statistically significant co-localization between accessible chromatin and regulatory variants across multiple layers of transcriptional control, with intronic and intergenic elements serving as predominant targets of cis-regulatory activity in porcine muscle.

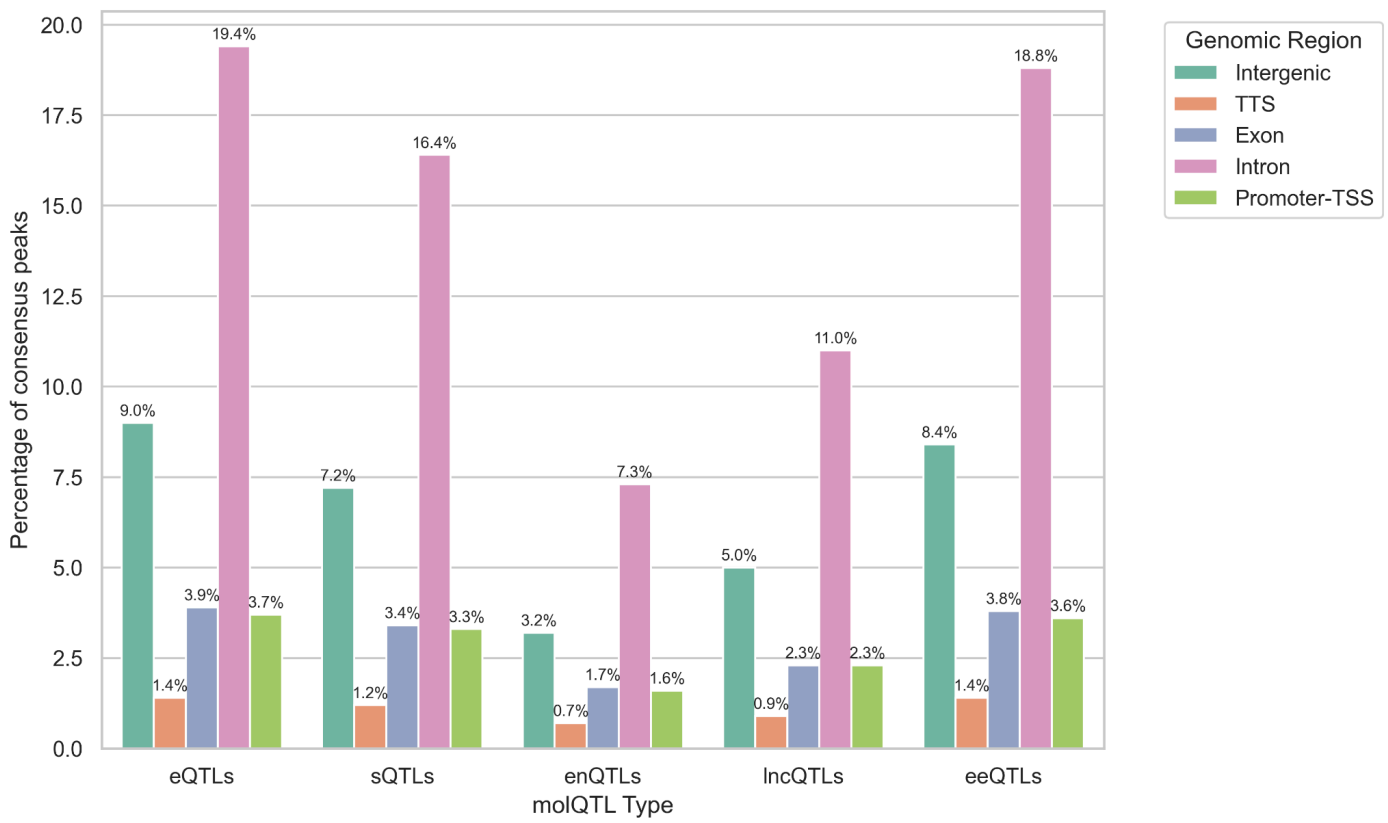

Figure 4. Genomic annotation of consensus ATAC-seq peaks overlapping with cis-regulatory molQTLs in porcine skeletal muscle. Bars represent the percentage of consensus peaks overlapping with eQTLs, sQTLs, enQTLs, lncQTLs, and eeQTLs, subdivided by genomic region. For all molQTL types, the number of overlapping variants was significantly greater than expected by chance based on 1,000 permutations (empirical $p < 0.001$).

3.3.2. Integration of DAPs between fetus and piglet with molQTLs

To assess how developmental changes in chromatin accessibility are associated with regulatory variants, we next examined the overlap of DAPs and molQTLs at the fetal and piglet stages.

A total of 25,008 (15.4%) DAPs with higher accessibility in fetuses and 25,725 (15.8%) DAPs with higher accessibility in piglets overlapped with at least one cis-eQTL region, corresponding to 153,325 and 141,374 eQTLs and 26,768 and 24,633 eGenes, respectively (Suppl. Table 5B). Although the total number of overlapping peaks was comparable between developmental stages, promoter/TSS-associated DAPs exhibited a notable asymmetry, both in the percentage of DAPs overlapping eQTLs (2.2% in fetus vs. 1.0% in piglet) and in the number of associated genes (1,948 vs. 716) that were both annotated by HOMER and classified as eGenes, indicating a stronger regulatory signal in promoter regions during fetal muscle development (Figure 5).

Overlap patterns for sQTLs followed a similar trend. Among DAPs, 21,146 (13.0%) fetal-accessible and 21,750 (13.4%) piglet-accessible peaks overlapped with 120,160 and 109,868 sQTL variants, respectively. Intronic regions were again the most frequently represented, with 5.7% fetal and 8.0%

piglet intronic peaks overlapping sQTLs. Promoter-TSS associated sQTL overlaps were more frequent in fetal peaks (1.9%) than in piglet peaks (0.9%).

The eeQTLs were found in 24,261 (14.9%) fetal-accessible and 25,001 (15.4%) piglet-accessible peaks, overlapping with 145,795 and 135,630 variants, respectively. Again, introns and intergenic regions were predominant, while 3,500 (2.2%) fetal and 1,537 (0.9%) piglet promoter peaks overlapped with eeQTLs.

The integration with lncQTLs identified 14,731 (9.1%) fetal-accessible and 14,560 (8.9%) piglet-accessible peaks overlapping with 72,808 and 64,702 lncQTL variants, respectively. Intronic and intergenic annotations remained the most common, while 2,196 (1.4%) fetal versus 947 (0.6%) piglet promoter-associated peaks overlapped with lncQTLs.

Finally, in the case of enQTLs, 10,101 (6.2%) fetal-accessible peaks and 9,543 (5.9%) piglet-accessible peaks overlapped with 49,518 and 42,394 enQTL variants, respectively. The majority of these were intronic (4,392 in fetus; 5,502 in piglet), followed by intergenic, exonic, and promoter/TSS-associated regions. Promoter-overlapping peaks showed 1,523 (0.9%) overlaps in fetal samples versus 690 (0.4%) in piglets.

Across all molQTL types, permutation-based enrichment tests confirmed that the observed number of variant overlaps in both fetal and piglet-accessible peaks was significantly greater than expected by chance (empirical $p < 0.001$).

These results showed that chromatin regions with developmental stage-specific accessibility were significantly enriched in multiple classes of cis-regulatory variants. The annotation patterns of these regions suggest differential regulatory engagement between stages: fetal-accessible regions showed higher counts in promoter and intergenic compartments, while piglet-accessible regions were more represented in intronic contexts.

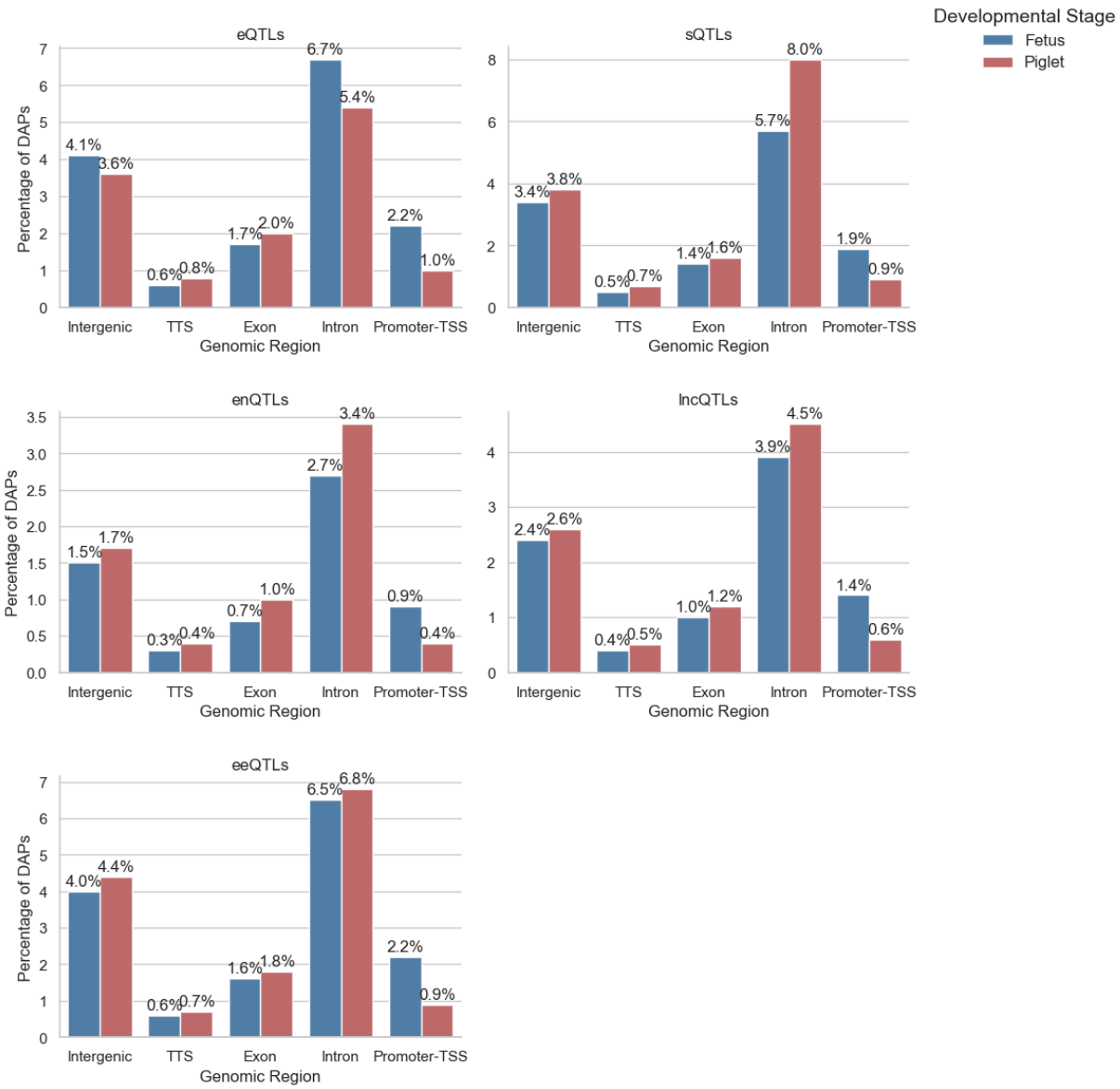

Figure 5. Stage-specific distribution of differentially accessible peaks (DAPs) overlapping molQTLs. Bar plots show the percentage of fetal and piglet-accessible DAPs that overlap molQTLs, subdivided by genomic annotation and stratified by molQTL type (eQTL, sQTL, eeQTL, enQTL, lncQTL). For all molQTL types and both developmental stages, the number of overlapping variants was significantly greater than expected by chance based on 1,000 permutations (empirical $p < 0.001$).

3.3.3 Enrichment of strong-effect molQTL variants in differentially accessible peaks

Next, we asked whether chromatin accessibility changes preferentially coincide with strong-effect molQTLs across the five classes of molecular QTLs tested. For each dataset, the strongest 25% of variants were defined based on absolute effect size. Although only a minority of all strong molQTLs overlapped DAPs (~6–9.5%, depending on molQTL type), a substantial fraction of the molQTLs present within DAPs were strong-effect variants (~32–52%). Enrichment analysis confirmed that strong molQTLs were significantly more likely than expected to coincide with DAPs in both fetal and piglet muscle (odds ratios 1.1–1.2; $p < 10^{-67}$ to $p < 10^{-235}$; Suppl. Table 7). These results indicate that

accessibility differences between developmental stages harbour strong-effect regulatory variants across multiple molecular QTL types.

Then we examined the genomic distribution of these strong-effect variants within DAPs (Figure 6). Intronic regions accounted for the majority of overlaps across all molQTL types, with ~43–57% of strong variants and a consistent piglet bias (~56% vs ~43% in fetus). Promoter–TSS regions, although representing a smaller proportion (~8–17%), showed a pronounced fetal bias, with significantly more strong-effect variants in fetuses than in piglets. Additional differences were also detected in intergenic, exon, and TTS categories for selected molQTL classes.

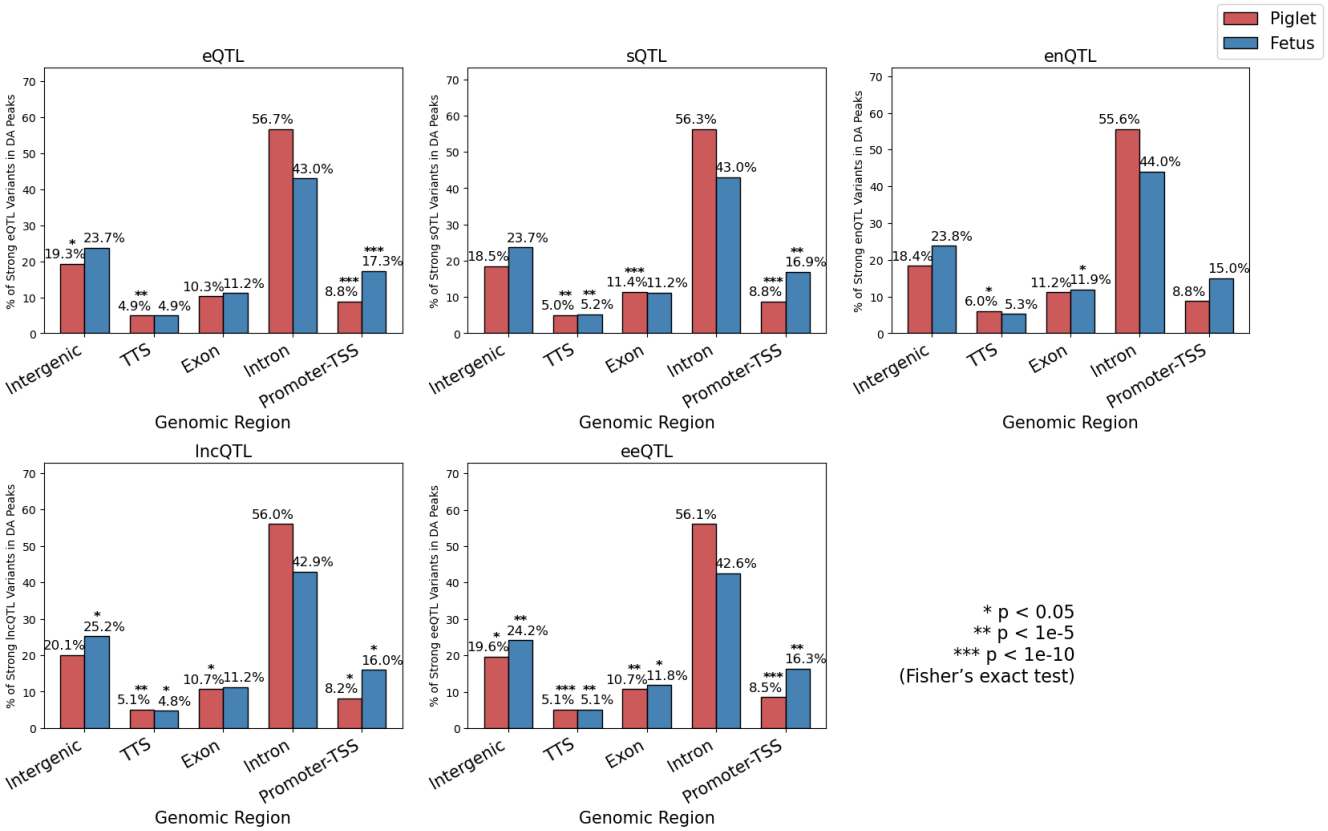

Figure 6. Genomic distribution of strong-effect molQTL variants within differentially accessible peaks. Barplots show the percentage of strong variants (top 25% by absolute effect size) for each molQTL type: eQTL, sQTL, enQTL, lncQTL, and eeQTL, found within differentially accessible (DA) chromatin regions in fetal (blue) and piglet (red) muscle. Genomic categories include intergenic, transcription termination site (TTS), exon, intron, and promoter–TSS regions. Asterisks indicate significant enrichment differences between fetal and piglet within each category based on Fisher's exact test ($p < 0.05$, p < 1e–5, p < 1e–10).

We finally focused on the top 1% strongest eQTLs ranked by effect size overlapping promoter–TSS DAPs. As shown in Figure 7, only four variants were located in promoter peaks more accessible in piglets, while the majority of variants (14 out of 18) overlapped promoter peaks more accessible in fetuses.

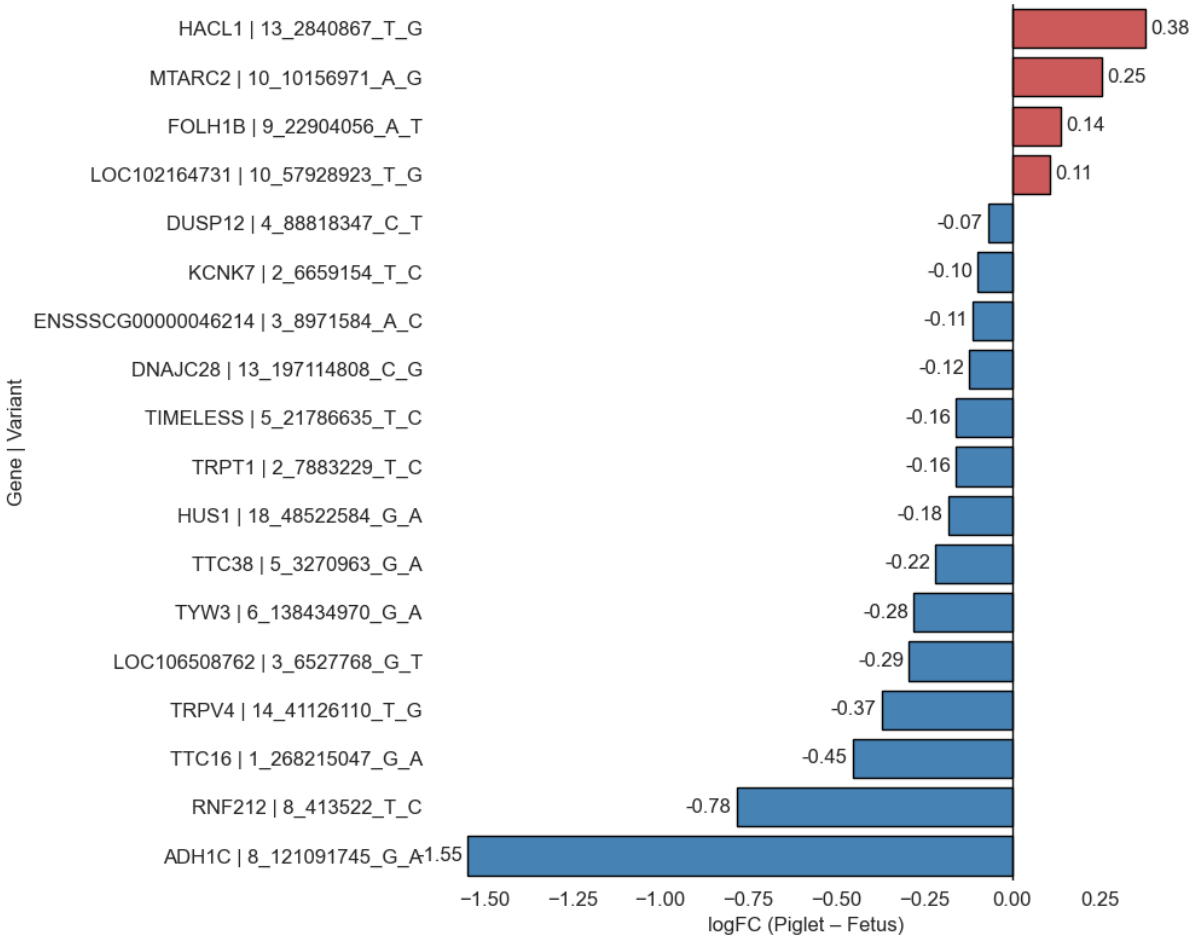

Figure 7. Accessibility bias of promoter-TSS eQTLs with the strongest effect. Barplots show logFC (Piglet vs. Fetus) in promoter accessibility for the top 1% strongest-effect eQTLs. Four variants overlap promoter peaks more accessible in piglets, while 14 overlap peaks more accessible in fetuses, indicating a predominant fetal bias.

Taken together, these results highlighted that the strongest cis-regulatory events shifted between the fetal and postnatal stages: from gene-distal and promoter-linked control in the fetal stage toward intragenic regulation at the postnatal stage.

3.4 Exploratory GO term enrichment of promoter associated eGenes

To investigate the potential biological functions of genes associated with promoter-accessible regions linked to cis-eQTLs, we performed a Gene Ontology (GO) enrichment analysis separately for fetal- and piglet-accessible gene sets. We focused in particular on GO Biological Process categories with uncorrected p-values < 0.05, fold enrichment > 1.5, and minimum gene counts ≥3 to identify possible functional trends.

Genes associated with fetal-accessible peaks linked to cis-eQTLs (n = 1,948) were enriched for RNA metabolic processes, chromosome organization, DNA repair, and ribosome biogenesis, reflecting active transcriptional and biosynthetic programs likely supporting cell proliferation and differentiation during prenatal muscle development. In contrast, piglet-accessible genes linked to cis-eQTLs (n = 716) were enriched for striated muscle contraction, lipid modification, cellular

respiration, and musculoskeletal movement, consistent with the metabolic and contractile functions of postnatal skeletal muscle (Suppl. Table 5).

Notably, several terms were unique to only one developmental stage. For instance, striated muscle contraction was enriched in piglet-specific genes alone, whereas regulation of organelle organization and chromosome organization were observed exclusively in the fetal set. These differences highlight how regulatory accessibility at promoters mark distinct functional states aligned with developmental transitions in muscle (Figure 8).

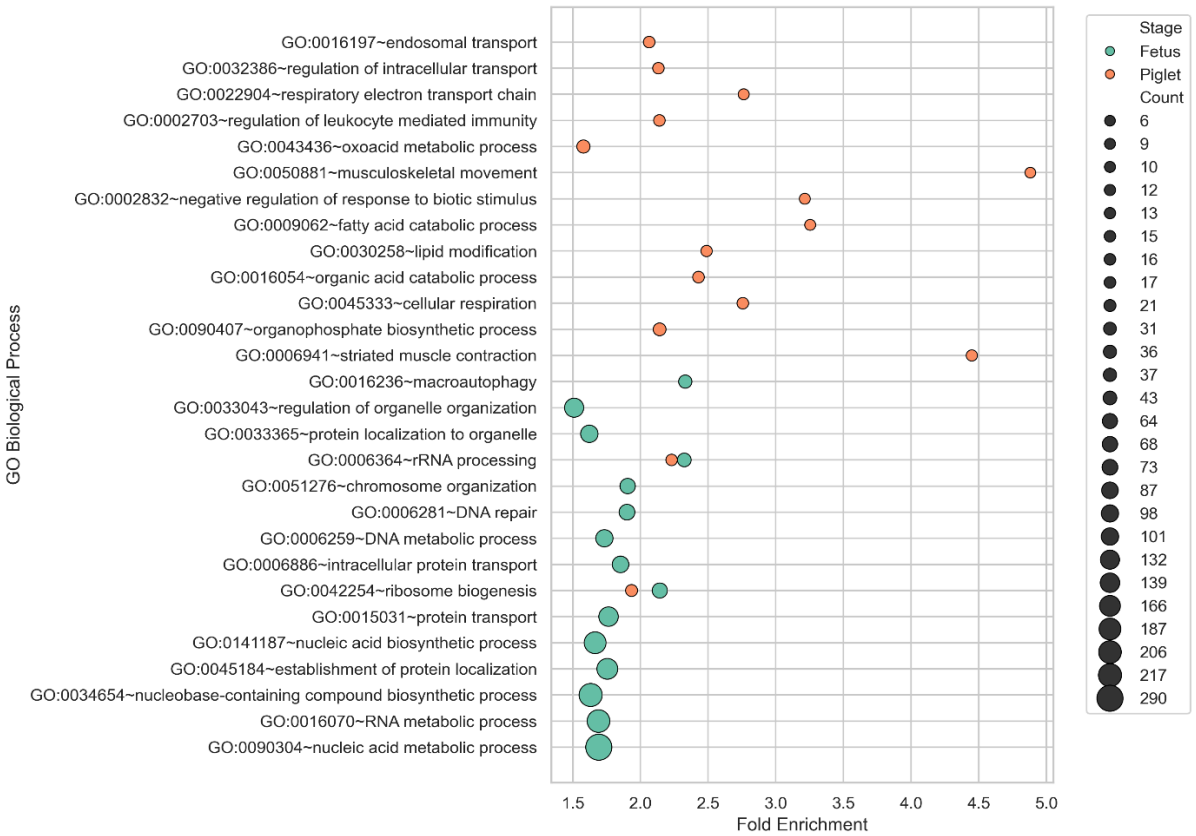

Figure 8. Exploratory GO term enrichment of promoter-associated eGenes in fetal and piglet skeletal muscle. Top 15 GO Biological Process (BP) terms per developmental stage enriched among genes linked to promoter-accessible, cis-eQTL-overlapping peaks. Dot size reflects gene count; X-axis shows fold enrichment. Terms shown passed filters of p-value < 0.05, fold enrichment > 1.5, and ≥ 3 genes. The figure highlights exploratory functional differences between prenatal and postnatal muscle chromatin accessibility.

3.5 Trait associations of promoter-accessible eGenes via GWAS colocalization

We used colocalized gene–trait associations from Xu et al. (2025), restricted to pairs with RCP > 0.5, to determine which complex traits were linked to fetal- or piglet-stage regulatory elements. Specifically we intersected the colocalized gene–trait pairs with our dataset of promoter-associated eGenes to identify which of the genes implicated in trait variation show developmental stage–specific chromatin accessibility at their promoters.

We identified 107 fetal-stage and 30 piglet-stage promoter-accessible eGenes colocalized with the same set of 10 complex traits including growth-related (backfat thickness, BFT; average daily gain, ADG; days to reach weight, DAYS), muscle structure (loin muscle area, LMA; loin muscle depth, LMDEP; lean cut percentage, LEANCUTP), and reproduction (number born alive, NBA; number born healthy, NBH; total number born, TNB; total litter weight at birth, TLWT_BA). Despite convergence at the trait level, the overlap of fetal and piglet genes was limited, with only three shared eGenes (ENSSSCG00000005663, ENSSSCG00000005935, ENSSSCG00000014060). Thus, while both developmental stages were connected to the same set of complex traits, the underlying gene sets associated with promoter accessibility are largely distinct between them.

Figure 9 further illustrates how trait associations distribute across developmental stages and GWAS data from different breeds. As expected, cross-breed analyses (M_) captured a broad set of growth, muscle, and reproduction traits consistently detected at both fetal and piglet stages, while within-breed analyses highlighted lineage-specific associations (e.g., Duroc for BFT at both stages, Landrace for NBA/TNB in fetus, and Yorkshire for TLWT_BA at both stages). Interestingly, Yorkshire showed a relatively high overlap of traits between stages, compared to more stage-restricted signals in Duroc and Landrace.

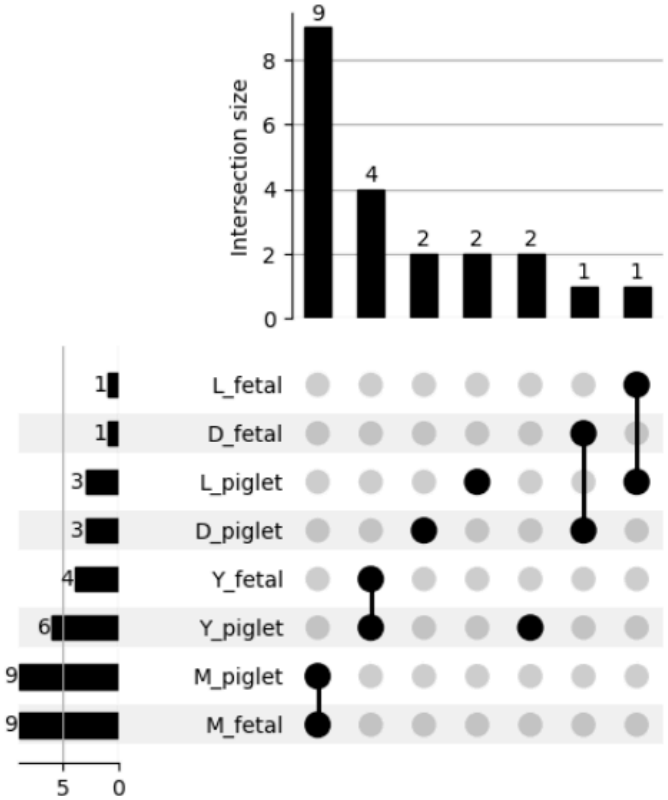

Trait	Groups
D_ADG	D_piglet
D_BFT	D_fetal, D_piglet
D_LMDEP	D_piglet
L_ADG	L_fetal, L_piglet
L_NBA	L_piglet
L_TNB	L_piglet
M_ADG	M_fetal, M_piglet
M_BFT	M_fetal, M_piglet
M_DAYS	M_fetal, M_piglet
M_LEANCUTP	M_fetal, M_piglet
M_LMA	M_fetal, M_piglet
M_LMDEP	M_fetal, M_piglet
M_NBA	M_fetal, M_piglet
M_NBH	M_fetal, M_piglet
M_TNB	M_fetal, M_piglet
Y_ADG	Y_fetal, Y_piglet
Y_DAYS	Y_fetal, Y_piglet
Y_LMDEP	Y_fetal, Y_piglet
Y_NBA	Y_piglet
Y_NBH	Y_piglet
Y_TLWT_BA	Y_fetal, Y_piglet

Figure 9. Intersection of colocalized trait associations with promoter-accessible eGenes across developmental stages and pig populations. UpSet plot showing the number and identity of traits associated with promoter-accessible eGenes colocalized with GWAS loci in fetal and piglet muscle. Traits are grouped by developmental stage (Fetus or Piglet) and by GWAS population label. The M_ prefix refers to traits derived from cross-breed meta-analyses (integrating data across 59 pig populations), while D_, L_, and Y_ indicate within-breed meta-analyses in Duroc, Landrace, and

Yorkshire pigs, respectively. The plot highlights the distribution of shared and stage-specific trait associations.

4. Discussion

By integrating high-quality ATAC-seq datasets across developmental stages and from different breeds, we generated a robust and generalizable map of the muscle chromatin accessibility landscape, which served as the foundation for downstream analyses of differential accessibility and regulatory variant integration using the PigGTEx resource.

Our differential accessibility analysis revealed extensive remodeling of the porcine muscle regulatory landscape between fetal and postnatal stages, with over 130,000 peaks showing significant developmental differences. The observation that fetal muscle exhibits greater accessibility at promoter and intergenic regions likely reflects the broad transcriptional priming and enhancer activity required to support active myogenesis. In contrast, the enrichment of intronic accessibility in piglet muscle suggests a shift toward regulatory refinement within gene bodies that accompanies fiber hypertrophy and metabolic specialization after birth (**Figure 3**). These patterns are consistent with previous studies performed in cattle (Cao et al., 2021), mouse (Dos Santos et al., 2023) and yak (Li et al., 2024). Previous studies in pigs have reported dynamic stage-specific accessibility. Yue et al. (2021) and Hou et al. (2025) showed that fetal muscle is enriched for promoter-proximal and intergenic open chromatin, supporting developmental gene regulation, while Feng et al. (2023) and Tan et al. (2025) demonstrated that postnatal muscle has fewer accessible peaks overall and a relative enrichment in intronic regions, in line with functional specialization of mature muscle.

The fact that a considerable proportion of consensus peaks overlap with all molQTL classes, with more than one-third overlapping with eQTLs, confirms that chromatin accessibility provides a useful proxy for identifying functional noncoding variants (**Figure 4**). Previous studies in cattle (Yuan et al., 2023), mice (Keele et al., 2020), and chickens (Zhu et al., 2023) have reported similar findings, where substantial fractions of eQTLs and other regulatory variants are enriched within open chromatin regions identified by ATAC-seq or DNase-seq, reinforcing the utility of chromatin accessibility as a cross-species marker of functional regulatory variation. The predominance of intronic and intergenic overlap highlights that the majority of functional regulatory variants act outside of proximal promoters, consistent with enhancer-mediated and distal regulation. Similar enrichments of QTLs in distal elements have been reported in pigs (Teng et al., 2024) and other species like cattle (Liu et al., 2022) and chickens (Pan et al., 2023) across multiple tissues supporting the notion that molecular trait variation is frequently mediated by open chromatin. Importantly, our permutation tests confirmed that the overlap of molQTLs with accessible chromatin was highly significant across all classes (empirical p-value < 0.001), indicating that these co-localizations are unlikely to arise by chance and that open chromatin is a consistent hotspot for functional regulatory variants.

The integration of molQTLs with the differentially accessible chromatin regions highlighted how cis-regulatory variants engage the distinct regulatory compartments across development (**Figure 5, Figure 6)**. Although the overall number of molQTL overlaps was similar between fetal and piglet-accessible peaks, fetal regions showed higher counts in promoter and intergenic categories, whereas piglet regions were more frequently represented in intronic contexts. This pattern is in full agreement with the functional signatures of prenatal transcriptional plasticity and postnatal

metabolic specialization previously reported in porcine transcriptomic and chromatin studies (Yue et al., 2021; Feng et al., 2023; Hou et al., 2025).

Promoter-associated eGenes were preferentially involved in RNA metabolism, DNA repair, and chromosomal organization, processes that align with the high proliferative and transcriptional activity required during myogenesis. In contrast, piglet-associated genes were related to striated muscle contraction, lipid metabolism, and cellular respiration, consistent with the metabolic and contractile demands of postnatal skeletal muscle. The presence of stage-specific terms, such as chromosome organization in fetal samples and striated muscle contraction in piglets, underscored how promoter accessibility may demarcate developmental transitions in muscle biology (**Figure 8**). When focusing on the top 1% of strongest-effect eQTLs located in promoter–TSS DAPs ranked by accessibility shifts (**Figure 7**), we observed that the majority of strong eQTLs coincided with promoters more accessible in fetal muscle, whereas only a minority aligned with piglet-biased promoters. This pronounced fetal bias suggests that high-effect eQTLs are preferentially embedded in regulatory elements active during fetal muscle development, possibly reflecting the higher transcriptional plasticity of the developing tissue.

The finding that both fetal and piglet promoter-accessible eGenes colocalize with the same set of 12 complex traits indicated that developmental stages converge on common phenotypic outcomes related to growth and muscle structure, in addition to participating to the phenotypic outcomes of other physiological functions (i.e., blood parameters and reproduction). However, the observation that only three eGenes were shared between the two stages highlights how these associations are mediated by distinct genes. This reinforces the idea that accessibility changes at promoters can shift which genes influence key traits without altering the overall functional domains under selection. Moreover, trait associations were unevenly distributed across developmental stages and GWAS data from different breeds (**Figure 9**). An open question is whether these patterns might be influenced by differences in genetic heterogeneity across the datasets. Cross-breed meta-analyses integrate diverse haplotype backgrounds, potentially revealing a wider range of variants and pathways shared across development, while within-breed analyses may emphasize more homogeneous, lineage-specific signals. Although our data are consistent with this possibility, further work would be needed to determine the extent to which genetic heterogeneity drives the observed differences.

Overall, these results suggest that identifying open chromatin regions is a promising initial step towards pinpointing regulatory variants that act at different developmental stages. Looking to the future, combining our growing understanding of the functional regulatory features of farmed animal genomes with advanced analytical tools for predicting the phenotypic effects of variants (e.g., Nguyen et al., 2025) will enable us to identify causative regulatory variants and their phenotypic impacts throughout development.

5. References

- Alexandre, P. A., Naval-Sánchez, M., Menzies, M., et al. (2021). Chromatin accessibility and regulatory vocabulary across indicine cattle tissues. *Genome Biology, 22*, 273. https://doi.org/10.1186/s13059-021-02489-7

· Bai, J., Lin, Y., Zhang, J., Chen, Z., Wang, Y., Li, M., & Li, J. (2023). Profiling of Chromatin Accessibility in Pigs across Multiple Tissues and Developmental Stages. International Journal of Molecular Sciences, 24(13), 11076. https://doi.org/10.3390/ijms241311076

· Buenrostro, J. D., Giresi, P. G., Zaba, L. C., Chang, H. Y., & Greenleaf, W. J. (2013). Transposition of native chromatin for fast and sensitive epigenomic profiling of open chromatin, DNA-binding proteins and nucleosome position. *Nature Methods, 10*(12), 1213–1218. https://doi.org/10.1038/nmeth.2688

Cao, X., Cheng, J., Huang, Y., Lan, X., Lei, C., & Chen, H. (2021). Comparative enhancer map of cattle muscle genome annotated by ATAC-seq. *Frontiers in Veterinary Science, 8*, 782409. https://doi.org/10.3389/fvets.2021.782409

· Chalabi, S., Loonen, L., Boekhorst, J., Li, H., Fang, L., Harrison, P. W., Lakhal, W., Lluch, J., Sokolov, A., Djebali, S., Rau, A., Giuffra, E., & Wells, J. (2025). Differences in maternal diet fiber content influence patterns of gene expression and chromatin accessibility in fetuses and piglets. *Genomics, 117*(2), 110995. https://doi.org/10.1016/j.ygeno.2025.110995

· Cho, I.-C., Park, H.-B., Ahn, J. S., Han, S.-H., Lee, J.-B., Lim, H.-T., et al. (2019). A functional regulatory variant of MYH3 influences muscle fiber-type composition and intramuscular fat content in pigs. PLOS Genetics, 15(10), e1008279. https://doi.org/10.1371/journal.pgen.1008279

· Clark, E. L., Archibald, A. L., Daetwyler, H. D., Groenen, M. A. M., Harrison, P. W., et al. (2020). From FAANG to fork: Application of highly annotated genomes to improve farmed animal production. *Genome Biology, 21*, 285. https://doi.org/10.1186/s13059-020-02197-8

· Crespo-Piazuelo, D., Acloque, H., Gonzalez-Rodriguez, O., et al. (2022). Identification of transcriptional regulatory variants in pig duodenum, liver, and muscle tissues. *GigaScience, 12*, giad042.https://doi.org/10.1093/gigascience/giad042

Dos Santos, M., Shah, A. M., Zhang, Y., et al. (2023). Opposing gene regulatory programs governing myofiber development and maturation revealed at single nucleus resolution. *Nature Communications, 14*, 4333. https://doi.org/10.1038/s41467-023-40073-8

· Ewels, P. A., Peltzer, A., Fillinger, S., Patel, H., et al. (2020). The nf-core framework for community-curated bioinformatics pipelines. *Nature Biotechnology, 38*(3), 276–278. https://doi.org/10.1038/s41587-020-0439-x

Fang, L., Teng, J., Lin, Q., et al. (2025). The Farm Animal Genotype–Tissue Expression (FarmGTEx) Project. *Nature Genetics, 57*, 786–796. https://doi.org/10.1038/s41588-025-02121-5

· Feng, L., Si, J., Yue, J., Zhao, M., Qi, W., Zhu, S., Mo, J., Wang, L., Lan, G., & Liang, J. (2023). The Landscape of Accessible Chromatin and Developmental Transcriptome Maps

Reveal a Genetic Mechanism of Skeletal Muscle Development in Pigs. International Journal of Molecular Sciences, 24(7), 6413. https://doi.org/10.3390/ijms24076413

· GENE-SWitCH Consortium. (2023). Functional annotation of porcine genome regulatory elements: Insights from GENE-SWitCH. *Ensembl Regulatory Build Documentation*. Available at: https://data.faang.org/projects/GENE-SWitCH

Harrison, P. W., Amode, M. R., Austine-Orimoloye, O., Azov, A. G., Barba, M., Barnes, I., Becker, A., Bennett, R., Berry, A., Bhai, J., ... (2024). Ensembl 2024. *Nucleic Acids Research, 52*(D1), D891–D899. https://doi.org/10.1093/nar/gkad1049

· Heinz, S., Benner, C., Spann, N., Bertolino, E., et al. (2010). Simple combinations of lineage-determining transcription factors prime cis-regulatory elements required for macrophage and B cell identities. *Molecular Cell, 38*(4), 576–589. https://doi.org/10.1016/j.molcel.2010.05.004

· Hou, X., Niu, N., Liu, X., Wang, L., Wang, L., & Zhang, L. (2025). Dynamic changes in chromatin accessibility and gene expression involved in fetal myogenesis of Min pig. *Animal Bioscience*. Advance online publication. https://doi.org/10.5713/ab.25.0034

Keele, G. R., Quach, B. C., Israel, J. W., Chappell, G. A., Lewis, L., et al. (2020). Integrative QTL analysis of gene expression and chromatin accessibility identifies multi-tissue patterns of genetic regulation. *PLOS Genetics, 16*(1), e1008537. https://doi.org/10.1371/journal.pgen.1008537

· Lawrence, M., Huber, W., Pages, H., Aboyoun, P., Carlson, M., et al. (2013). Software for computing and annotating genomic ranges. *PLoS Computational Biology, 9*(8), e1003118. https://doi.org/10.1371/journal.pcbi.1003118

Li, H., & Durbin, R. (2009). Fast and accurate short read alignment with Burrows-Wheeler transform. *Bioinformatics, 25*(14), 1754–1760. https://doi.org/10.1093/bioinformatics/btp324

Li, J., Chen, Z., Bai, Y., Wei, Y., Guo, D., Liu, Z., Niu, Y., Shi, B., Zhang, X., Cai, Y., Zhao, Z., Hu, J., Wang, J., Liu, X., Li, S., & Zhao, F. (2024). Integration of ATAC-Seq and RNA-Seq analysis to identify key genes in the longissimus dorsi muscle development of the Tianzhu White Yak. *International Journal of Molecular Sciences, 25*(1), 158. https://doi.org/10.3390/ijms25010158

· Lin, H., Peng, H., Sun, Y., et al. (2023). Reprogramming of cis-regulatory networks during skeletal muscle atrophy in male mice. Nature Communications, 14, 6581. https://doi.org/10.1038/s41467-023-42313-3

· Liu, R., Holik, A. Z., Su, S., Jansz, N., Chen, K., Leong, H. S., et al. (2015). Why weight? Modelling sample and observational level variability improves power in RNA-seq analyses. *Nucleic Acids Research, 43*(15), e97. https://doi.org/10.1093/nar/gkv412

Liu, S., Gao, Y., Canela-Xandri, O., Wang, S., Yu, Y., Cai, W., … Fang, L. (2022). A multi-tissue atlas of regulatory variants in cattle. *Nature Genetics, 54*(9), 1438–1447. https://doi.org/10.1038/s41588-022-01153-5

· Lun, A. T., & Smyth, G. K. (2016). csaw: A Bioconductor package for differential binding analysis of ChIP-seq data using sliding windows. *Nucleic Acids Research, 44*(5), e45. https://doi.org/10.1093/nar/gkv1191

· Miao, W., Ma, Z., Tang, Z., Yu, L., Liu, S., Huang, T., Wang, P., Wu, T., Song, Z., Zhang, H., Li, Y., & Zhou, L. (2021). Integrative ATAC-seq and RNA-seq analysis of the longissimus muscle of Luchuan and Duroc pigs. *Frontiers in Nutrition, 8*, 742672. https://doi.org/10.3389/fnut.2021.742672

· Nguyen, D.T., Knutsen, T.M., Sandve, S.R., Lien, S. & Grønvold, L. 2025. "Sequence-Based Chromatin Activity Modeling and Regulatory Impact Prediction of Genetic Variants in Farmed Animals Using Deep Learning." NAR Genomics and Bioinformatics 7 (4). https://doi.org/10.1093/nargab/lqaf139

· Pan, Z., Zhou, Y., He, S., Liu, H., Han, R., Zhang, H., … Li, N. (2023). An atlas of regulatory elements in chicken: A resource for chicken genetics and genomics. *Science Advances, 9*(18), eade1204. https://doi.org/10.1126/sciadv.ade1204

· Salavati, M., Woolley, S. A., Cortés Araya, Y., Halstead, M. M., Stenhouse, C., Johnsson, M., Ashworth, C. J., Archibald, A. L., Donadeu, F. X., Hassan, M. A., & Clark, E. L. (2022). Profiling of open chromatin in developing pig (*Sus scrofa*) muscle to identify regulatory regions. *G3: Genes|Genomes|Genetics, 12*(2), jkab424. https://doi.org/10.1093/g3journal/jkab424

· Sosnicki, A., Gonzalez, J., Fields, B., & Knap, P. (2025). A review of porcine skeletal muscle plasticity and implications for genetic improvement of carcass and meat quality. *Meat Science, 219*, 109676. https://doi.org/10.1016/j.meatsci.2024.109676

· Tan, W., Liu, C., Liu, J., Wen, S., Chen, Y., Ren, R., Gao, N., Ding, X., He, J., & Zhang, Y. (2025). Integrative Analysis of ATAC-Seq and RNA-Seq Identifies Key Genes Affecting Muscle Development in Ningxiang Pigs. *International Journal of Molecular Sciences*, *26*(6), 2634. https://doi.org/10.3390/ijms26062634

· Teng, J., Gao, Y., Yin, H. *et al.* A compendium of genetic regulatory effects across pig tissues. *Nat Genet* 56, 112–123 (2024). https://doi.org/10.1038/s41588-023-01585-7

· Xu, Z., Lin, Q., Cai, X., Zhong, Z., Teng, J., Li, B., Zeng, H., Gao, Y., Cai, Z., Wang, X., Shi, L., Wang, X., Wang, Y., Zhang, Z., Lin, Y., Liu, S., Yin, H., Bai, Z., Wei, C., ... Zhang, Z. (2025). Integrating large-scale meta-GWAS and PigGTEx resources to decipher the genetic basis of 232 complex traits in pigs. *National Science Review, 12*(5), nwaf048. https://doi.org/10.1093/nsr/nwaf048

· Yuan, C., Tang, L., Lopdell, T., Petrov, V. A., Oget-Ebrad, C., Moreira, G. C. M., Gualdrón Duarte, J. L., Sartelet, A., Cheng, Z., Salavati, M., Wathes, D. C., Crowe, M. A., GplusE Consortium, Coppieters, W., Littlejohn, M., Charlier, C., Druet, T., Georges, M., & Takeda, H. (2023). An organism-wide ATAC-seq peak catalog for the bovine and its use to identify regulatory variants. *Genome Research, 33*(10), 1848–1864. https://doi.org/10.1101/gr.277947.123

· Yue, J., Hou, X., Liu, X. et al. The landscape of chromatin accessibility in skeletal muscle during embryonic development in pigs. J Animal Sci Biotechnol 12, 56 (2021). https://doi.org/10.1186/s40104-021-00577-z

Zhang, Y., Liu, T., Meyer, C. A., Eeckhoute, J., Johnson, D. S., Bernstein, B. E., Nusbaum, C., Myers, R. M., Brown, M., Li, W., & Liu, X. S. (2008). Model-based analysis of ChIP-Seq (MACS). *Genome Biology, 9*, R137.https://doi.org/10.1186/gb-2008-9-9-r137

Zhu, X.-N., Wang, Y.-Z., Li, C., Wu, H.-Y., Zhang, R., & Hu, X.-X. (2023). Chicken chromatin accessibility atlas accelerates epigenetic annotation of birds and gene fine-mapping associated with growth traits. *Zoological Research, 44*(1), 53–62. https://doi.org/10.24272/j.issn.2095-8137.2022.228

6. Acknowledgements

E. Shishmani was supported by a PhD grant in Agricultural Technologies and Biotechnologies (Curriculum: Welfare, Biotechnology and Quality of Animal Production).